Soft Matter

Accepted Manuscript

This article can be cited before page numbers have been issued, to do this please use: T. R. Weikl, *Soft Matter*, 2026, DOI: 10.1039/D6SM00343E.

ROYAL SOCIETY OF CHEMISTRY

rsc.li/soft-matter-journal

View Article Online
DOI: 10.1039/D6SM00343E

Journal Name

ARTICLE TYPE

Cite this: DOI: 00.0000/xxxxxxxxxx

Membrane tubulation by spherical nanoparticles: Effect of lateral tension

Thomas R. Weikl

Received Date
Accepted Date

DOI: 00.0000/xxxxxxxxxx

Adhesion of spherical nanoparticles or virus-like particles to membranes can lead to membrane tubules in which linear chains of adhering particles are cooperatively wrapped by the membrane. This cooperative wrapping of spherical particles in tubules is energetically favourable compared to the individual wrapping of the particles because of a favourable interplay of membrane bending and particle adhesion energies in the membrane necks that connect the particles to the neighbouring particles in the tubule. In this article, we investigate how the energy gain for the cooperative wrapping of spherical nanoparticles in tubules is affected by lateral membrane tension as well as by the membrane thickness, which limits the radius of the membrane necks between the particles. We find that membrane tension tends to stabilize weakly undulated tubule shapes at intermediate particle adhesion energies, but only moderately affects the energy gain of cooperative wrapping at larger adhesion energies. For tight membrane necks limited by the membrane thickness, however, the energy gain of cooperative wrapping can vanish if the range of the particle adhesion potential is too small to still lead to a favourable interplay of bending and adhesion energies in these necks.

1 Introduction

Cellular uptake of nanoparticles can occur via a variety of endocytic pathways [1,2], which all require the generation of cell membrane curvature and membrane invaginations. Nanoparticles that adhere to cell membranes can themselves generate membrane curvature if their adhesion energy is sufficiently large to compensate for the cost of membrane bending [3]. The nanoparticles then can be partially or fully wrapped by the membrane, depending on their shape and size [4,5], the bending rigidity and tension of the membrane [6], the energy and range of the adhesion potential [7], and the curvature of the plasma membrane segment or membrane vesicle prior to wrapping [8,9] in the interplay of the elastic energy of the membrane and the adhesion energy of the particles.

Nanoparticles can also be cooperatively wrapped as linear chains of particles in membrane tubules, besides being wrapped individually as single particles. In computational approaches, cooperative wrapping of spherical nanoparticles in membrane tubules has been both found in Monte Carlo simulations in which the membranes are modelled as triangulated elastic surfaces [10,11] and in coarse-grained molecular simulations of particle-membrane systems [12–16]. In experiments, cooperative wrapping in membrane tubules has been observed for spherical citrate-stabilized gold nanoparticles with a diameter of 10 nm in contact with POPC or DOPC large unilamellar vesicles [17] (see Figure 1a). The gold nanoparticles are arranged linearly with a distance of about 3 nm in the membrane tubules, which protrude into the vesicle interior and exhibit periodic shaping of the membrane around the wrapped particles [17]. Particle-induced membrane tubulation of cells has been first reported for spherical virus-like particles with a diameter of 45 nm that are composed of capsid proteins binding to GM1 glycolipids in the cell membranes (see Figure 1c) [18]. The particles are linearly arranged in the cell membrane tubules, with varying distances between the particles (see arrows in Figure 1c). More recently, the role of the particle adhesion energy for cell membrane tubulation has been explored in an artificial system of capsid particles that are densely covered with green fluorescent proteins (GFPs) and bind to anti-GFP nanobodies anchored to the cell membranes (see Figure 1d) [19]. In this system, the particle adhesion energy was varied by using a repertoire of anti-GFP nanobodies with different affinities for GFP. For nanobodies with affinities beyond a threshold value, membrane tubulation was observed both for energy-depleted cells and giant unilamellar vesicles (GUVs) in fluorescence micrographs. High-resolution electron microscopy images correlated with fluorescence recordings indicate membrane tubules filled by particle chains (see Figure 1e). Pairs of rod-shaped particles with a length of several micrometers have been observed to be cooperatively wrapped in tubular membrane invaginations of GUVs with a tip-to-tip orientation of the particles [20]. In this system, particle adhesion to GUVs was induced by depletion interactions from non-adsorbing polyacrylamide polymers in the solvent. For micron-sized spherical particles adhering to GUVs via specific biotin-

Max Planck Institute of Colloids and Interfaces, Department of Biomolecular Systems, Potsdam Germany. E-mail: thomas.weikl@mpikg.mpg.de

View Article Online
DOI: 10.1039/D6SM00343E

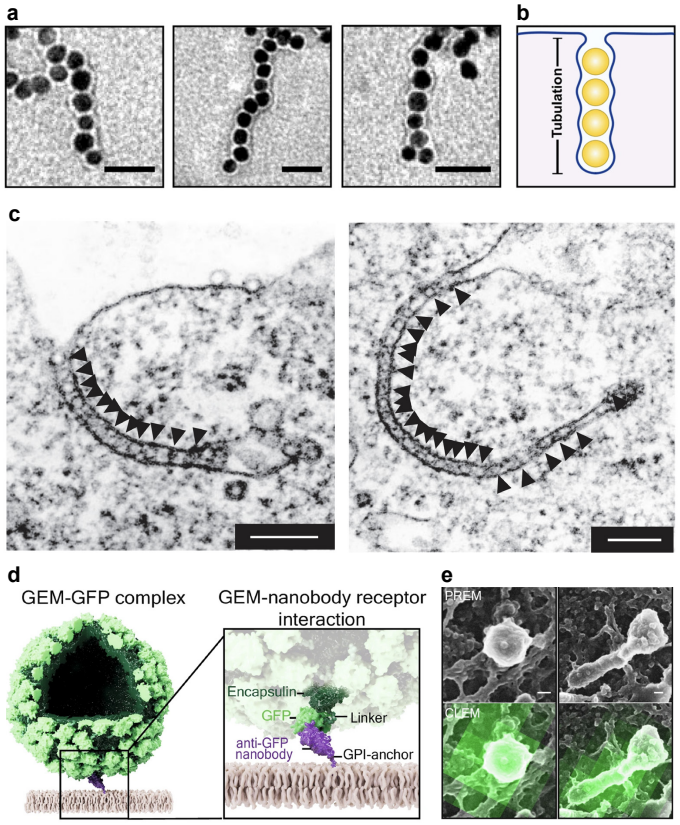

Fig. 1 (a) Linear chains of citrate-stabilized gold nanoparticles with a diameter of about 10 nm in membrane tubules of large unilamellar vesicles. The scale bars of the transmission electron microscopy pictures are 50 nm. The particle-filled membrane tubules protrude into the vesicle interior as sketched in (b). Reproduced with permission from Ref. 17. (c) Linear chains of virus-like particles with a diameter of 45 nm (highlighted by triangular arrows) in tubular membrane invaginations of cells. The scale bar of the electron micrographs are 200 nm. The particles are composed of 72 icosahedrally organized capsid protein pentamers that contain a binding site for cell membrane GM1 glycolipids in each monomer. Control experiments indicate that the membrane invaginations are induced by particle adhesion without the help of active endocytic machinery or caveolar coats[18]. Reproduced with permission from Ref. 18. (d) Illustration of a genetically encoded nanoparticle (GEM) assembled from encapsulin proteins in the artificial adhesion system of Ref. 19. The particles are densely covered by GFP proteins coupled to the encapsulin proteins and bind to anti-GFP nanobodies anchored to the cell membranes. (e) Platinum-replica electron microscopy (PREM) and correlative light electron microscopy (CLEM) pictures of plasma membrane sheets generated after unroofing cells in contact with GEMs. The elongated green fluorescent structure on the right indicates a short GEM-filled membrane nanotube. The GEMs are not wrapped and internalized by endocytic events involving clathrin-coated pits or caveolae according to control experiments. The scale bars are 50 nm. Reproduced with permission from Ref. 19.

avidin repector-ligand interactions, tube-like structures in which two particles are cooperatively wrapped have been observed as a rather rare conformation among other dimer conformations[21,22].

The cooperative wapping of nanoparticles observed in these computational and experimental systems implies an energy gain for the wrapping of linear chains of particles in membrane tubules, compared to the individual wrapping of the particles as single particles. For spherical nanoparticles, the energy gain of cooperative wrapping in membrane tubules has been found to depend strongly on the interaction range of the adhesion potential relative to the particle radius, and to vanish if the interaction range becomes negligibly small[7]. In energetic arguments[3,8], in energy calculations based on the shape equations of rotationally symmetric membrane vesicles[6,9], and in energy minimizations[23] with the popular "Surface Evolver"[24] software, the interaction range of particles adhering to membranes is often assumed to be zero for computational convenience or necessity, because a zero potential range allows a sharp distinction between adhering and non-adhering membrane segments. However, the assumption of zero potential range is only a valid approximation in determining the membrane-wrapping behavior of spherical particles if the particle radius is at least three orders of magnitude larger than the interaction range of the particle-membrane adhesion potential[7], so, e.g., for micron-sized particles with short-ranged adhesive interactions on the length scale of a nanometer. For a potential range of zero, spherical particles are fully wrapped by a tensionless, initially planar membranes as soon as the bending energy cost $8\pi\kappa$ of full wrapping is compensated by the adhesion energy $-4\pi r_m^2 U$ where κ is the bending rigidity of the membrane, $-U$ is the adhesion energy per area, and r_m is the radius of the spherical membrane vesicle wrapping the particle[3,25]. The spherical vesicle around the particle is connected to the surrounding planar membrane by a membrane neck of catenoidal shape, which does not contribute to the overall bending energy because the mean curvature of the catenoid is zero. Similarly, energy calculations for wrapping chains of particles at zero range of the particle-membrane adhesion potential predict full wrapping of the particles beyond the threshold adhesion energy $U = 2\kappa/r_m^2$, with catenoidal necks connecting the particles[25]. At zero potential range, the overall energy $4\pi n(2\kappa - r_m^2 U)$ of wrapping n particles individually by a tensionless membrane or cooperatively as chain of particles therefore is the same. This calculation implies that also the membrane thickness and, thus, the catenoidal neck limited by this thickness, is negligibly small compared to the vesicle membrane radius r_m.

At realistic finite potential ranges, in contrast, adhering and non-adhering membrane segments of a spherical nanoparticle are separated by a finite contact region in which the membrane detaches from the particle. In this contact region, the membrane already “swings into” the catenoidal shape of the surrounding non-adhering membrane, but still gains adhesion energy, which leads to a favourable contribution to the overall energy of wrapping[7]. The energy gain for the cooperative wrapping of spherical particles in membrane tubules then simply results from the fact that a central particle in a membrane tubule has two of these energetically favourable contact regions in the membrane necks to the neighbouring particles, compared to a single contact region for an individually wrapped particle in the neck to the surrounding non-adhering membrane (see Figure 2).

For elongated particles, e.g. prolate or sphero-cylindrical, rod-shaped particles, cooperative wrapping in membrane tubules with tip-to-tip orientation provides an energy gain compared to the individual wrapping of the particles also for negligibly small ranges of the adhesion potential[26]. For these particles, the wrapping of

View Article Online
DOI: 10.1039/D6SM00343E

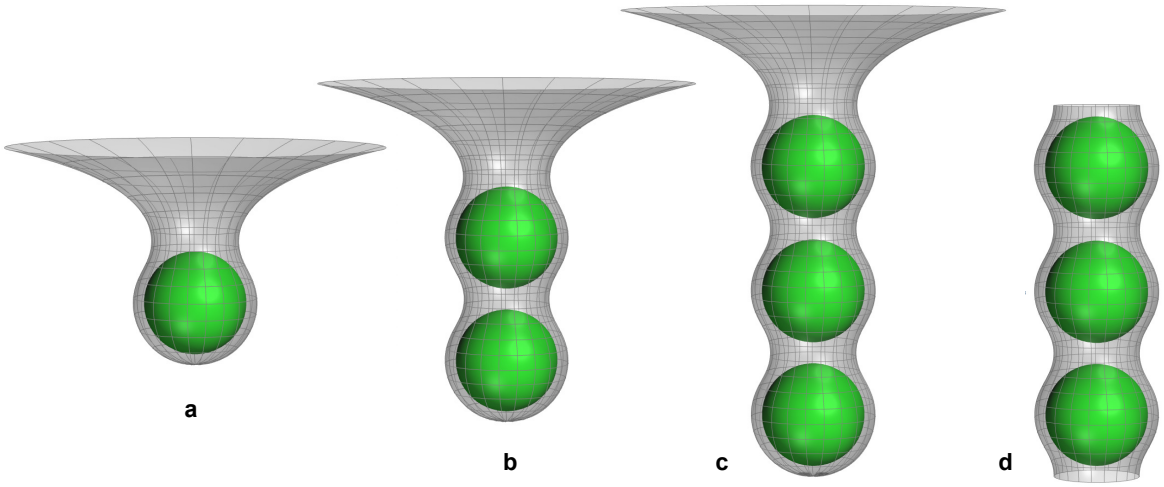

Fig. 2 Minimum-energy conformations of (a) a single spherical particle, (b) two particles, (c) three particles, and (d) three central particles in a linear chain of many particles wrapped by a tensionless membrane for the rescaled adhesion energy $u = 2.5$, particle radius $r_p = 19$ nm, vesicle membrane radius $r_m = 23$ nm, and standard deviation $\xi = 1$ nm of the particle membrane adhesion potential (2). The rotationally symmetric membrane shapes in (b) and (c) have been constructed from segments of the numerically determined shapes in (a) and (d).

the highly curved tips costs more bending energy per area than the wrapping of the less curved sides, and the wrapping in membrane tubules is energetically favourable because both tips of a central particle in the tubule remain unwrapped. In line with these predictions based on minimizations of the sum of bending and adhesion energies, micron-sized rod-shaped particles have been observed to have a strong tendency to be cooperatively wrapped tip-to-tip by membrane tubules[20], whereas micron-sized spherical particles with an adhesion potential range that is several orders of magnitude smaller than the particle diameter exhibit tube-like structures in which two particles are cooperatively wrapped only as a rather rare conformation among other dimer conformations[21,22]. For spherocylindrical nanoparticles, cooperative wrapping by membrane tubules with tip-to-tip orientation of the particles has also been reproduced in coarse-grained molecular simulations[27].

In this article, we revisit and extend the elastic model of Ref. 7 for the cooperative wrapping of spherical particles in tubules (i) by including membrane tension and (ii) by considering the radius of tight membrane necks, which are limited by the membrane thickness, and the particle radius r_p as length parameters in addition to the adhesion potential range and the membrane vesicle radius r_m. For a fully wrapped spherical particle, the membrane tension τ leads to the energy contribution $4\pi r_m^2 \tau$ that needs to be compensated by the adhesion energy of the particle, in addition to the bending energy cost $8\pi\kappa$ of full wrapping (see above). The membrane tension τ therefore increases the adhesion energy required for particle wrapping[6]. At sufficiently large adhesion energies for wrapping, we find that the energy gain ΔE of cooperative wrapping per particle is only weakly affected by the membrane tension. For large particle adhesion energies at which the particles are fully wrapped and connected by tight membrane necks in tubules, however, the energy gain ΔE of cooperative wrapping vanishes if the range of the particle adhesion potential is too small to still lead to a favourable interplay of bending and adhesion energies in these necks.

2 Methods

2.1 Elastic model

The membrane curvature generation and wrapping of adhesive particles results from the interplay of the elastic energy of the membrane and the adhesion energy of the particles. The total energy E is the sum

$$E = E_{\rm be} + \tau\Delta A + E_{\rm ad} \tag{1}$$

of the membrane bending energy $E_{\rm be} = 2\kappa \int M^2 \,{\rm dA}$ with local mean curvature M, the adhesion energy $E_{\rm ad} = \int \sum_{i=1}^{n_p} V(l_i) {\rm d}A$ of the membrane in contact with n_p particles, and the energy $\tau\Delta A$ associated with the membrane tension τ, where ΔA is the excess area of the curved membrane relative to initially planar membrane prior to particle adhesion. The particle-membrane adhesion potential $V(l)$ depends on the local distance l of the membrane midplane from a particle surface and is described here by the Gaussian potential

$$V(l) = -Ue^{-(l-l_o)^2/2\xi} \tag{2}$$

where $-U$ is the adhesion energy per area, l_o is the preferred binding separation of the membrane midplane from the particle surface, and ξ is the standard deviation of the Gaussian function that reflects the range of the adhesion potential. The Gaussian potential (2) is plausible if the particle adhesion is mediated by receptor and ligand molecules that are flexibly anchored to the particles and the membrane[28]. The preferred binding separation l_o and standard deviation ξ of the adhesion potential then depend on the dimensions of the receptor-ligand complex, which can tilt due to the flexible anchoring, and the lengths of the flexible linkers that anchor the receptors and ligands, and the adhesion energy $-U$ per area depends on the ligand density on the particle surface and the binding constant of the receptor-ligand

View Article Online
DOI: 10.1039/D6SM00343E

interaction[19] (see Supplementary Information for details).

Three central length parameters of the model are the particle radius r_p, the radius $r_m = r_p + l_o$ of membrane segments that wrap the particle at the preferred binding separation l_o, and the standard deviation ξ of the adhesion potential (2). Besides the membrane radius r_m, the particle radius r_p is a relevant parameter for the cooperative wrapping in membrane tubules because it limits the distance $d \geq 2r_p$ of particles in tubules. A fourth length scale of the model is the membrane thickness, which sets a lower limit for the radius of the catenoidal membrane necks. For a tight catenoidal neck in which the membrane segments lining the neck are in contact, the minimum neck radius for the midplane of these membrane segments is about half the membrane thickness.

Besides these length parameters, two central dimensionless parameters of the model are the rescaled adhesion energy

$$u = U r_m^2/\kappa \tag{3}$$

and the rescaled tension

$$\gamma = \tau r_m^2/\kappa \tag{4}$$

which can be derived from the three energetic parameters U, κ, and τ by understanding the bending rigidity κ as energy unit and the membrane radius r_m as length unit in approaches focussing on minimum total energies as here.

2.2 Energy minimization

To determine the minimum-energy shapes of the rotationally symmetric membranes around individually wrapped particles or cooperatively wrapped linear chains of particles, we extend the methodology of Ref. 7 to membranes under tension. In this methodology, we discretize the profiles of the rotationally symmetric membrane shapes in two different parametrizations. In parametrization 1, the rotationally symmetric membrane shapes are described by the function $r(z)$ where z is the coordinate along the axis of rotation, and r is the radial distance from this axis. We use parametrization 1 to determine the membrane shapes around central particles in membrane tubules with distance $d \geq 2r_p$ between the particles as well as the rotationally symmetric membrane shape around a single, deeply wrapped particle, e.g. the left shape of Figure 2. To determine the rotationally symmetric membrane shape around particles that are less than half-wrapped by the membrane, we use parametrization 2 in which the membrane profile is described by the function $z(r)$. We numerically obtain the minimum-energy shapes by discretising the functions $r(z)$ and $z(r)$ of the two parametrizations and by determining the function values at the discretization points in constrained energy minimizations with the program Mathematica 14.3 (see Supplementary Information for details).

3 Results

We first consider the cooperative wrapping of linear chains of particles in membrane tubules, with a focus on how the rotationally symmetric minimum-energy membranes shapes and particle distances of the tubules depend on the rescaled membrane tension γ and the rescaled adhesion energy u of the particles defined in eqs. (3) and (4). We initially adjust the length parameters of our model to the particle system of Fig. 1d (see Supplementary Information for details), but consider later the effect of these length parameter values on the results. Figure 3 illustrates how the conformations of the particle-filled membrane tubules depend on the rescaled adhesion energy u for tensionless membranes with $\gamma = 0$ already considered in Ref. 19 and for membranes with rescaled tension $\gamma = 0.2$, 0.5, and 1. Two central quantities to describe the tubule conformations are the distance d of the particles and the radius r_n of the membrane midplane in the center of the membrane neck between the particles. At the value $u = U r_m^2/\kappa = 2$ at which the adhesion energy $-4\pi r_m^2 U$ of a spherical vesicle with radius r_m fully wrapping a single particle at preferred separation l_o of the adhesion potential (2) is oppositely equal to the bending energy $8\pi\kappa$ of the vesicle, the particles are in contact in the tubule with distance $d = 2r_p$ between the particles (see Fig. 3c), and the membrane tubules are only weakly undulated with a neck radius r_n larger than $0.8r_m$. Here, r_m is the membrane-midplane radius of membrane segments wrapping the particle at preferred separation l_o and, thus, the maximum radius of the tubules at cross sections that contain the particle centres. For $\gamma = 0$ and 0.2, the tubule conformations change continuously with increasing u (see Fig. 3a for $\gamma = 0.2$). At these values of γ, the particle distance d starts to increase continuously with u at the transition values $u_t \simeq 2.41$ for $\gamma = 0$ and $u_t \simeq 2.69$ for $\gamma = 0.2$. At large values of u, the tubule conformations are strongly undulated and attain the minimum neck radius $r_n = 2.5$ nm for the membrane thickness 5 nm assumed here (gray dashed line at $r_n/r_m = 2.5/23 \simeq 0.109$ in Fig. 2d). At the minimum neck radius, the neck is closed, i.e. the membrane segments lining the neck are in contact. At large values of u, the particle distance tends to $d \simeq 2.75r_p$, with a distance maximum at intermediate values around $u = 3.3$ (see Fig. 3d). For $\gamma = 0.5$ and 1, in contrast, the tubule conformations change discontinuously at the transition values $u_t \simeq 3.09$ and 3.54, respectively. At these transition values, the stable tubule conformation changes abruptly from weakly undulated to deeply undulated as illustrated in Fig. 3b for $\gamma = 1$. However, in the process of tubule formation, weakly undulated tubule shapes may persist as metastable conformations for rescaled adhesion energies u larger than the transition values u_t due to hysteresis in the discontinuous transition of the particle wrapping state[6].

Cooperative wrapping of linear chains of particles in membrane tubules requires an energetic gain compared to the individual wrapping of the particles. In Fig. 4a, the minimum total energy E per central particle of a long tubule is compared to the minimum total energy E of an individually wrapped particle. The data points in Fig. 4 represent minimization results, and the lines are interpolations of the data points. For particles in tubules, and for individually wrapped particles in tensionless membranes with $\gamma = 0$, the results obtained with our minimization methods are numerically precise at all values of the rescaled adhesion energy u. For individually wrapped particles in membranes under tension, the minimization methods are (i) numerically precise for particles that are less than half wrapped and (ii) numerically reliable for deeply wrapped particles, with numerical errors that are negligi-

View Article Online
DOI: 10.1039/D6SM00343E

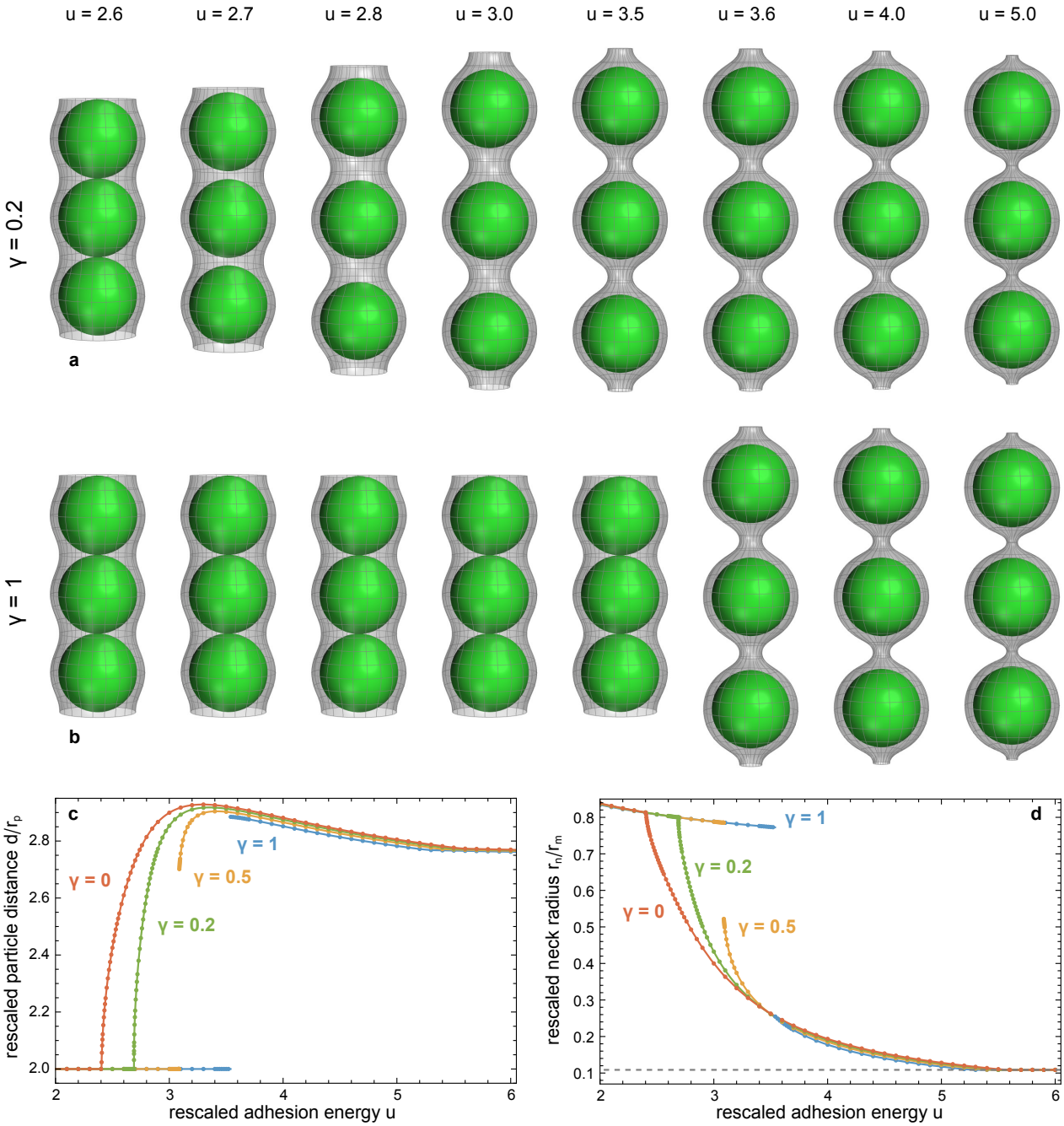

Fig. 3 (a) and (b) Minimum-energy conformations of three central particles in a membrane tubule wrapping many particles at the rescaled membrane tension $\gamma = 0.2$ and 1 at various values of the rescaled adhesion energy u. (c) Particle distance d and (d) neck radius r_n in a membrane tubule wrapping many particles versus rescaled adhesion energy u at the rescaled membrane tensions $\gamma = 0$, 0.2, 0.5, and 1. The particle radius here is taken to be $r_p = 19$ nm, the preferred distance of adhering membrane segments from the particle center is $r_m = 23$ nm, and the standard deviation of the particle membrane adhesion potential (2) is $\xi = 1$ nm (see Supplementary Information). The minimum neck radius of 2.5 nm for a membrane thickness of 5 nm is represented by the gray dashed line in (d).

View Article Online
DOI: 10.1039/D6SM00343E

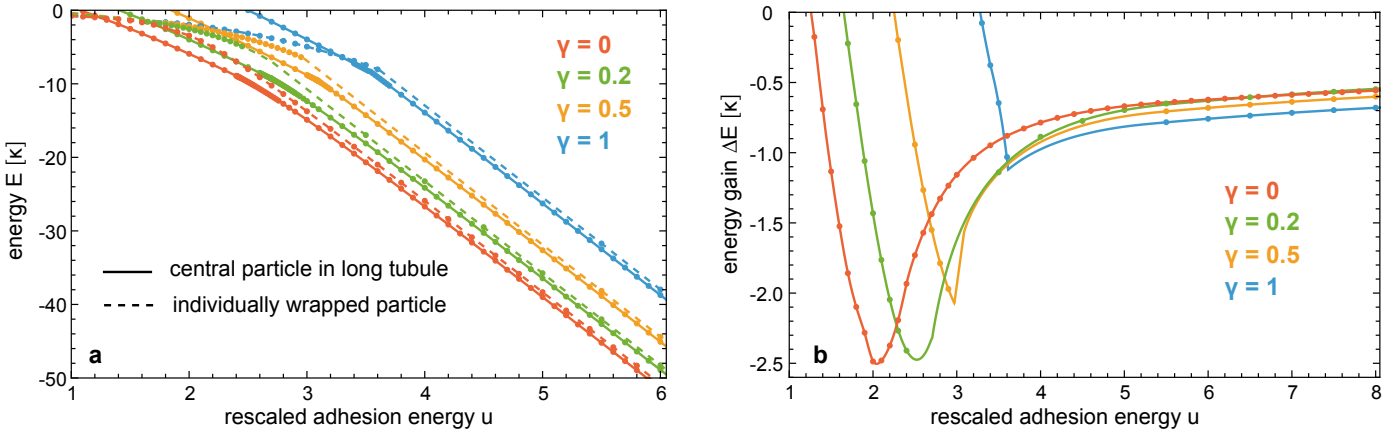

Fig. 4 (a) Total energy E of individually wrapped particles (points interpolated by dashed lines) and per central particle in long membrane tubule wrapping many particles (points interpolated by full lines) versus rescaled adhesion u at different values of the rescaled tension γ for the same parameter values as in Figure 3. (b) Energy gain ΔE per central particle in long membrane tubule relative to an individually wrapped particle versus rescaled adhesion u at different values of γ.

bly small compared to the values of the energy gain for cooperative wrapping considered below (see Supplementary Information for details). At intermediate values of u at which no minimization results are available, we interpolate the energies from the results obtained in the regimes (i) and (ii). These interpolations benefit from the linear dependence of the energy E on large values of u in regime (ii). In regime (i), we fit the minimization data points by a cubic function, which is extended in the dashed interpolation lines in Fig. 4 for $\gamma > 0$ until the intersection point with the linear fit obtained in regime (ii). The interpolation lines in Fig. 4 can be taken as guides for the eye connecting the data points, which are obtained directly from energy minimizations.

At sufficiently large rescaled adhesion energies u, the minimum total energy E per central particle of a long tubule is lower than the minimum total energy E of an individually wrapped particle (see Figure 4a). The resulting energy gain ΔE of cooperative wrapping, defined as difference of the two energies of Fig. 4a, is illustrated in Fig. 4b. For tensionless membranes with $\gamma = 0$, the energy gain ΔE of cooperative wrapping, relative to individual wrapping, is maximal close to $u = 2$ at which the adhesion energy of membrane segments adhering at preferred separation l_o of the adhesion potential (2) is oppositely equal to the bending energy of these segments (see above). At the value $u = 2$ of the rescaled adhesion energy, single particles are half wrapped by a tensionless membrane[7]. With increasing rescaled membrane tension γ, the energy ΔE attains its maximal value are larger and larger values of u, because the membrane tension impedes wrapping. At large values of u, the energy gain ΔE of membranes under tension is rather close to the energy ΔE for a tensionless membrane, in particular at the rescaled tensions $\gamma = 0.2$ and 0.5. At these large values of u, individual particles as well as particles in tubules are rather deeply wrapped by the membrane, and connected to the non-adhering membrane and the adjacent particles in the tubule, respectively, by membrane necks (see Figures 2 and 3).

As previously shown for tensionless membranes[7], the energy gain for the cooperative wrapping in tubules results from a favourable interplay of elastic and adhesion energies in the contact regions in which the membrane detaches from the particle. In this contact region, the membrane already "swings" into the catenoidal shape of the tensionless membrane neck, but still gains adhesion energy because of the finite range of the adhesion potential. The energy gain of cooperative wrapping then simply results from the fact that a central particle in a membrane tubule has two of these energetically favourable contact regions in the membrane necks to the two neighbouring particles, compared to a single neck and, thus, single contact region of an individually wrapped particle. The interplay of elastic and adhesion energies in these contact regions can be understood from the energy densities $e(z)$, $e_{\rm be}(z)$, $e_{\rm ad}(z)$ of the total energy, bending energy, and adhesion energy, which are integrated over the coordinate z along the axis of rotation to obtain the corresponding energies E, $E_{\rm be}$, and $E_{\rm ad}$ of eq. (1) (see Supplementary Information for details and illustrations of energy densities).

We finally consider how the membrane conformations and the energy gain ΔE of cooperative wrapping in tubules are affected by the length parameters of our model, i.e. by the particle radius r_p, the standard deviation ξ of the adhesion potential (2), and the minimum radius r_n of membrane necks, relative to the radius r_m of membrane segments adhering at preferred particle-membrane separation, which can be taken as reference length or "length unit" in our continuum model. In Ref. 7, the particle radius r_p was taken to be equal to r_m, and the radius r_n of membrane necks was allowed to attain arbitrary small values. With these assumptions, the minimum-energy membrane shapes and the energy gain ΔE of cooperative wrapping only depend on the range of the adhesion potential relative to the membrane radius r_m, i.e. on the ratio ξ/r_m here, besides the dimensionless parameters u and γ defined in Eqs. (3) and (4). For tensionless membranes with $\gamma = 0$ as in Ref. 7, Figure 5a illustrates that the energy gain ΔE of cooperative wrapping in the particle system of Figure 1d modelled with $r_p = 19$ nm, minimum neck radius $r_n = 2.5$ nm, and membrane radius $r_m = 23$ nm clearly decreases when the

View Article Online
DOI: 10.1039/D6SM00343E

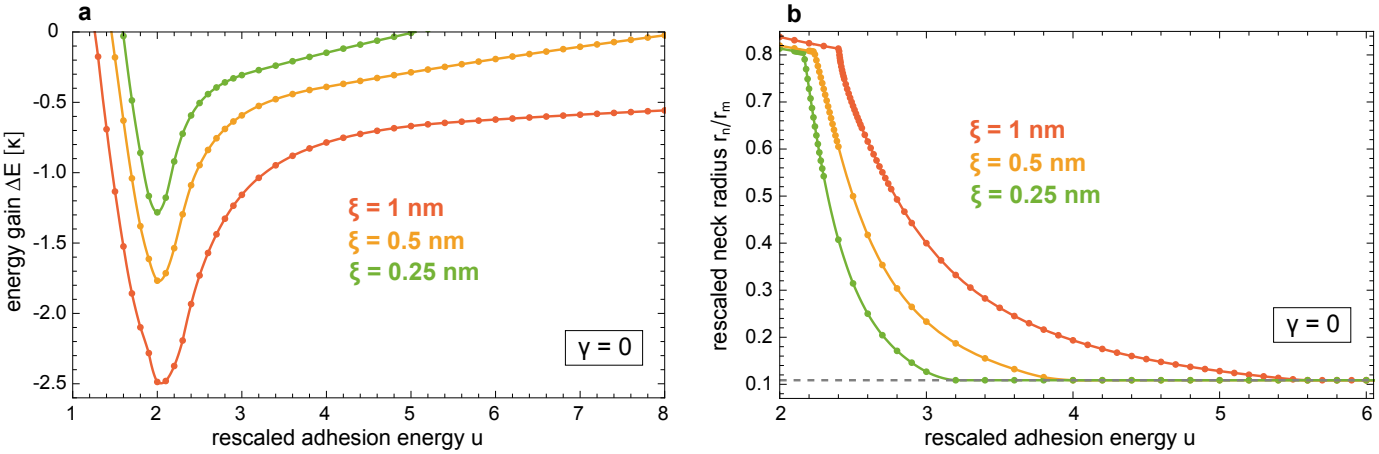

Fig. 5 (a) Energy gain ΔE per central particle in long membrane tubule relative to an individually wrapped particle and (b) rescaled neck radius r_n/r_m of membrane tubules versus rescaled adhesion u for tensionless membranes with rescaled tension $\gamma = 0$ and at the standard deviation $\xi = 1$ nm, 0.5 nm, and 0.25 nm of the adhesion potential (2).

standard deviation of the adhesion potential (2) is reduced from $\xi = 1$ nm to 0.5 nm and 0.25 nm. In contrast to Ref. 7, the energy gain vanishes, i.e. becomes non-negative, at large values of u for reduced potential ranges with $\xi = 0.5$ nm and $\xi = 0.25$ nm. Because the particles attain distances d in tubules clearly larger than the minimum value $2r_p$ determined by the particle radius r_p at large values of u, this difference to Ref. 7 can only result from the finite minimum value $r_n = 2.5$ nm of the neck radius. With decreasing potential range, the membrane tubules attain necks with minimum radius 2.5 nm already at smaller values of u (see Figure 5b). The vanishing energy gain at large u for reduced potential ranges can be understood by comparing the total energy densities e for the finite minimum value $r_n = 2.5$ nm of the neck radius to total energy densities with unconstrained neck radii as in Ref. 7 (see Supplementary Information for details and illustrations of these energy densities).

In contrast to the minimum neck radius, which affects the model results at large values of u, the particle radius r_p only affects the results at smaller values of u in Figure 3c at which the particles distance d is equal to the minimum distance $2r_p$ or only slightly larger. At larger values of u, the tubule conformations are not constrained by the length parameter r_p. For an intermediate range of rescaled adhesion energies u in which the particle distance in the tubules is clearly larger than r_p and in which the radius r_n of membrane necks is larger than the minimum value, the model results only depend on the ratio ξ/r_m as in Ref. 7.

4 Discussion and conclusions

In this article, we have extended previous modelling results[7,19] for the cooperative wrapping of linear chains of spherical nanoparticles in membrane tubules by considering how the minimum-energy shapes of the particle-filled tubules and the energy gain ΔE for the cooperative wrapping in tubules depend on the rescaled membrane tension γ and on various length parameters of the particles and membrane. The energy gain ΔE of cooperative wrapping is maximal at an intermediate value of the rescaled adhesion energy u at which individual particles are about half-wrapped by the membrane. For tensionless membranes, ΔE is maximal close to the value $u = 2$ at which the adhesion energy of a membrane segment adhering at optimal particle-membrane separation is oppositely equal to the bending energy of the segment. With increasing membrane tension, ΔE attains its maximal value at larger and larger values of u (see Figure 4b) because the membrane tension impedes wrapping, which needs to be compensated by the adhesion energy in addition to the bending energy cost of wrapping.

At large values of the rescaled adhesion energy u, the particles are deeply wrapped, and the energy gain ΔE for the cooperative wrapping in tubules is rather weakly affected by the membrane tension and increases only slightly with the rescaled tension γ up to the value $\gamma = 1$ (see Fig. 4). The rather small effect of the rescaled tension γ on the energy gain ΔE at large values of u can be understood from the crossover length $\zeta = \sqrt{\kappa/\tau} = r_m/\sqrt{\gamma}$ between bending-energy-dominated and tension-dominated elastic regimes. The elastic energy of the membrane is dominated by the bending energy on length scales smaller than the crossover length, and by the membrane tension τ on length scales larger than the crossover length[29]. For $\gamma = 1$, the crossover length ζ is equal to the radius r_m of membrane segments adhering at optimal separation l_o of the adhesion potential (2). For $\gamma = 0.2$ and $\gamma = 0.5$, the crossover length ζ is $5r_m$ and $2r_m$, respectively. At these values of γ, the crossover length ζ is clearly larger than the extension of the contact region in which the membrane detaches from a deeply wrapped particle. The elastic energy of this contact region, which leads to the energy gain ΔE, thus is dominated by the bending energy of the membrane. For the membrane radius $r_m = 23$ nm of the particle system in Fig. 1d and the typical bending rigidity value $\kappa = 30\, k_B T$[30,31], the rescaled tension $\gamma = 1$ corresponds to the membrane tension $\tau = \gamma\kappa/r_m^2 \simeq 0.2$ mN/m, which is a relatively large membrane tension that is only about one order of magnitude smaller than the maximally sustained tension at which membranes rupture[32]. For values of γ larger than 1, the tension-induced increase in the energy gain ΔE for cooperative wrapping at sufficiently large rescaled adhesion energies u

View Article Online
DOI: 10.1039/D6SM00343E

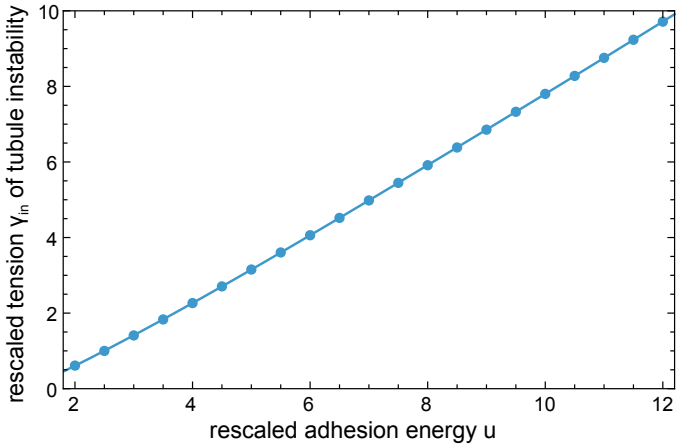

Fig. 6 Rescaled tension γ_{in} at which central particles of a long tubule contribute a minimum total energy of 0 for the same parameter values as in Figure 3. At γ_{in}, particle-filled tubules previously formed at lower rescaled tension γ become instable. The line represents the cubic fit function $\gamma_{in}(u) = -0.936 + 0.725\,u + 0.0222\,u^2 - 0.000726\,u^3$ of the data points.

becomes more pronounced because of an increase in the energy of the non-adhering membrane around a single particle (see Supplementary Information).

At small values of the rescaled adhesion energy u, the minimum total energy E of a particle in a membrane tubule becomes positive because the bending energy cost of the tubular membrane shape is no longer compensated by the adhesion energy gain (see Fig. 4a). Tubules, formed e.g. at smaller tension values, become instable at a rescaled tension γ_{in} that increases with increasing rescaled adhesion energy u (see Figure 6). For single particles fully wrapped by a vesicle membrane, tension-induced unwrapping has been observed after increasing the membrane tension by micropipette suction[33]. For a partially wrapped single particle, in contrast, the minimum total energy E is always negative (see Fig. 4a). At small values of u, the bending energy of cost of partial wrapping tends to 0 with decreasing u because the membrane approaches a planar shape, in which a particle "sitting" on the membrane still gains adhesion energy because of the finite range of the adhesion potential (2).

The energy gain ΔE for the cooperative wrapping of spherical particles strongly depends on the range of the adhesion potential, which determines the size of the contact region in which the membrane detaches from the particle with favourable interplay of bending and adhesion energies[7]. In addition to the potential range, another length scale that restricts the energy gain ΔE for cooperative wrapping at large rescaled adhesion energies u is the minimum radius of the membrane necks in the particle-filled tubules. For the particle system of Fig. 1d modelled with a standard deviation $\xi = 1$ of the adhesion potential (2), the energy gain ΔE is negative and, thus, favourable also at large values of u for the minimum neck radius $r_n = 2.5$ nm (see Figure 5a), in line with experiments in which the adhesion energy was varied by using nanobody receptors with vastly different affinities[19]. In these experiments, membrane tubulation was observed for all receptors with affinities beyond a threshold value.

In this article, we have focused on spherical particles adhering to initially planar membranes. For single particles, the curvature of the membrane prior to adhesion has been shown to affect the wrapping behaviour. For spherical polystyrene particles with diameters of about 1 and 2 μm that adhere to the outside of GUVs due to depletion interactions induced by polyethylene glycol (PEG) polymers in the surrounding solvent, an energetic barrier for particle wrapping has been observed[34], in line with theoretical calculations[8,9]. Monte Carlo simulations of several particles adhering to vesicles show that the membrane-mediated interactions of the particles that lead to tubule formation depend on the curvature of the vesicle membrane[35,36] and on the area-to-volume ratio of the vesicles[10]. Coarse-grained simulations of adhering spherical particles indicate that the membrane-mediated interactions are affected by the softness of the particles[37]. Also for mixtures of spherical particles with different diameters and adhesion energies, cooperative wrapping has been observed in simulations and experiments[38,39]

Conflicts of interest

There are no conflicts to declare.

Data availability

All Mathematica 14.3 notebooks used to generate and plot the data of this article are available in the open research data repository Edmond at https://doi.org/10.17617/3.OAPOLZ[40].

Acknowledgements

The author thanks the Max Planck Society for generous funding, and Amir Bahrami, Rumiana Dimova, Helge Ewers, Raluca Groza, Reinhard Lipowsky, and Michael Raatz for inspiring discussions in previous joint work on the article topic. The author is grateful to Erich Sackmann for his pioneering work on supported membranes[41] and on the specific adhesion of reconstituted vesicles by receptor-ligand complexes[42], which deeply affected the author's scientific path.

References

1 J. J. Rennick, A. P. R. Johnston and R. G. Parton, *Nat. Nanotechnol.*, 2021, **16**, 266–276.
2 M. Sousa de Almeida, E. Susnik, B. Drasler, P. Taladriz-Blanco, A. Petri-Fink and B. Rothen-Rutishauser, *Chem. Soc. Rev.*, 2021, **50**, 5397–5434.
3 R. Lipowsky and H. G. Döbereiner, *Europhys. Lett.*, 1998, **43**, 219–225.
4 A. H. Bahrami, *Soft Matter*, 2013, **9**, 8642–8646.
5 S. Dasgupta, T. Auth and G. Gompper, *Nano Lett.*, 2014, **14**, 687–693.
6 M. Deserno, *Phys. Rev. E*, 2004, **69**, 031903.
7 M. Raatz, R. Lipowsky and T. R. Weikl, *Soft Matter*, 2014, **10**, 3570–3577.
8 J. Agudo-Canalejo and R. Lipowsky, *ACS Nano*, 2015, **9**, 3704–3720.
9 A. H. Bahrami, R. Lipowsky and T. R. Weikl, *Soft Matter*, 2016, **12**, 581–587.

View Article Online
DOI: 10.1039/D6SM00343E

10 A. H. Bahrami, R. Lipowsky and T. R. Weikl, *Phys. Rev. Lett.*, 2012, **109**, 188102.
11 A. Saric and A. Cacciuto, *Phys. Rev. Lett.*, 2012, **109**, 188101.
12 T. Yue and X. Zhang, *ACS Nano*, 2012, **6**, 3196–3205.
13 K. Xiong, J. Zhao, D. Yang, Q. Cheng, J. Wang and H. Ji, *Soft Matter*, 2017, **13**, 4644–4652.
14 E. J. Spangler, P. B. S. Kumar and M. Laradji, *Soft Matter*, 2018, **14**, 5019–5030.
15 S. Zuraw-Weston, D. A. Wood, I. K. Torres, Y. Lee, L.-S. Wang, Z. Jiang, G. R. Lázaro, S. Wang, A. A. Rodal, M. F. Hagan, V. M. Rotello and A. D. Dinsmore, *Nanoscale*, 2019, **11**, 18464–18474.
16 E. J. Spangler and M. Laradji, *J. Chem. Phys.*, 2021, **154**, 244902.
17 C. Contini, J. W. Hindley, T. J. Macdonald, J. D. Barritt, O. Ces and N. Quirke, *Commun. Chem.*, 2020, **3**, 130.
18 H. Ewers, W. Roemer, A. E. Smith, K. Bacia, S. Dmitrieff, W. Chai, R. Mancini, J. Kartenbeck, V. Chambon, L. Berland, A. Oppenheim, G. Schwarzmann, T. Feizi, P. Schwille, P. Sens, A. Helenius and L. Johannes, *Nat. Cell Biol.*, 2010, **12**, 11–U36.
19 R. Groza, K. V. Schmidt, P. M. Müller, P. Ronchi, C. Schlack-Leigers, U. Neu, D. Puchkov, R. Dimova, C. Matthaeus, J. Taraska, T. R. Weikl and H. Ewers, *Nat. Commun.*, 2024, **15**, 2767.
20 S. van der Ham, J. Agudo-Canalejo and H. R. Vutukuri, *ACS Nano*, 2024, **18**, 10407–10416.
21 C. van der Wel, D. Heinrich and D. J. Kraft, *Biophys. J.*, 2017, **113**, 1037–1046.
22 C. van der Wel, A. Vahid, A. Saric, T. Idema, D. Heinrich and D. J. Kraft, *Sci. Rep.*, 2016, **6**, 32825.
23 S. Dasgupta, T. Auth and G. Gompper, *Soft Matter*, 2013, **9**, 5473–5482.
24 K. A. Brakke, *Exp. Math.*, 1992, **1**, 141–165.
25 A. H. Bahrami, M. Raatz, J. Agudo-Canalejo, R. Michel, E. M. Curtis, C. K. Hall, M. Gradzielski, R. Lipowsky and T. R. Weikl, *Adv. Colloid Interface Sci.*, 2014, **208**, 214–224.
26 M. Raatz and T. R. Weikl, *Adv. Mater. Interfaces*, 2017, **4**, 1600325.
27 A. Sharma, Y. Zhu, E. J. Spangler, J.-M. Y. Carrillo and M. Laradji, *Soft Matter*, 2023, **19**, 1499–1512.
28 J. Steinkühler, B. Rozycki, C. Alvey, R. Lipowsky, T. R. Weikl, R. Dimova and D. E. Discher, *J. Cell. Sci.*, 2019, **132**, jcs216770.
29 R. Lipowsky, in *Vesicles and Biomembranes*, Encyclopedia of Applied Physics, John Wiley & Sons, Ltd, 2003.
30 R. Dimova, *Adv. Colloid Interface Sci.*, 2014, **208**, 225–234.
31 J. F. Nagle, *Faraday Discuss.*, 2013, **161**, 11–29.
32 C. E. Morris and U. Homann, *J. Membr. Biol.*, 2001, **179**, 79–102.
33 F. Fessler, P. Muller and A. Stocco, *J. Colloid Interface Sci.*, 2025, **700**, 138524.
34 H. T. Spanke, R. W. Style, C. François-Martin, M. Feofilova, M. Eisentraut, H. Kress, J. Agudo-Canalejo and E. R. Dufresne, *Phys. Rev. Lett.*, 2020, **125**, 198102.
35 A. Vahid, A. Šarić and T. Idema, *Soft Matter*, 2017, **13**, 4924–4930.
36 A. Bahrami and A. H. Bahrami, *Nanotechnology*, 2019, **30**, 345101.
37 T. Chen, Y. Zhang, X. Li, C. Li, T. Lu, S. Xiao and H. Liang, *J. Chem. Theory Comput.*, 2021, **17**, 7850–7861.
38 K. He, Y. Wei, Z. Zhang, H. Chen, B. Yuan, H.-B. Pang and K. Yang, *Nanoscale*, 2021, **13**, 9626–9633.
39 Y. Wei, H. Chen, Y.-X. Li, K. He, K. Yang and H.-B. Pang, *ACS Nano*, 2022, **16**, 5885–5897.
40 T. Weikl, *Mathematica notebooks for article "Membrane tubulation by spherical nanoparticles: Effect of lateral tension"*, 2026, `https://doi.org/10.17617/3.OAPOLZ`.
41 E. Sackmann, *Science*, 1996, **271**, 43–8.
42 A. Albersdörfer, T. Feder and E. Sackmann, *Biophys. J.*, 1997, **73**, 245–257.

MAX PLANCK INSTITUTE
OF COLLOIDS
AND INTERFACES

MPI of Colloids and Interfaces • Am Mühlenberg 1 • 14476 Potsdam • Germany

Dr. Thomas Weikl
Group leader
Tel. +49 331 567-9608
thomas.weikl@mpikg.mpg.de

All Mathematica 14.3 notebooks used to generate and plot the data of this article are available in the open research data repository Edmond at https://doi.org/10.17617/3.OAPOLZ (see also Ref. 43).

Thomas Weikl